Archean Molecular Fossils and the Early Rise of Eukaryotes

Jochen J. Brocks *et al.*

Science **285**, 1033 (1999);
DOI: 10.1126/science.285.5430.1033

Science (print ISSN 0036-8075; online ISSN 1095-9203) is published weekly, except the last week in December, by the American Association for the Advancement of Science, 1200 New York Avenue NW, Washington, DC 20005.

Archean Molecular Fossils and the Early Rise of Eukaryotes

Jochen J. Brocks,[1,2]* Graham A. Logan,[2] Roger Buick,[1] Roger E. Summons[2]

Molecular fossils of biological lipids are preserved in 2700-million-year-old shales from the Pilbara Craton, Australia. Sequential extraction of adjacent samples shows that these hydrocarbon biomarkers are indigenous and syngenetic to the Archean shales, greatly extending the known geological range of such molecules. The presence of abundant 2α-methylhopanes, which are characteristic of cyanobacteria, indicates that oxygenic photosynthesis evolved well before the atmosphere became oxidizing. The presence of steranes, particularly cholestane and its 28- to 30-carbon analogs, provides persuasive evidence for the existence of eukaryotes 500 million to 1 billion years before the extant fossil record indicates that the lineage arose.

Microfossils (*1*), stromatolites (*2*), and sedimentary carbon isotope ratios (*3*) all indicate that microbial organisms inhabited the oceans in Archean times [>2500 million years ago (Ma)]. But these lines of evidence are not very informative about what these microbes were or how they lived. Potentially, a better insight into primordial biological diversity can be obtained from molecular fossils derived from cellular and membrane lipids ("biomarkers"). Although such soluble hydrocarbons were first extracted from Archean rocks more than 30 years ago, their significance was generally discounted after amino acids of recent origin were found in the same rocks (*4*). Prevailing models of thermal maturation dictated that complex hydrocarbons should not survive the metamorphism experienced by all Archean terrains. However, indications of greater hydrocarbon stability (*5*) and observations of oil in Archean fluid inclusions (*6*) suggest that these maturation models are unduly pessimistic and that biomarkers could indeed be preserved in low-grade Archean metasedimentary rocks. Furthermore, systematic sampling strategies, improved analytical techniques, and greater geochemical knowledge (*7*) should make their recognition easier and their interpretation more rigorous. We now report molecular fossils in late Archean shales that have suffered only minimal metamorphism. These molecular fossils reveal that the Archean biota was considerably more complex than currently recognized and that the domains Eucarya and Bacteria were already extant.

Samples came from depths of around 700 m in diamond drill core WRL#1, collared near Wittenoom in the Pilbara Craton of northwestern Australia (*8*). They represent the ~2600-Ma Marra Mamba Formation (*9*) (lowermost Hamersley Group), the underlying Roy Hill and Warrie Members of the ~2690-Ma Jeerinah Formation (*10*), and the ~2715-Ma Maddina Formation (Fortescue Group) (*9*), all of which have only been metamorphosed to prehnite-pumpellyite facies in this area (*11*) (~200° to ~300°C). The closely spaced sampling of different lithologies allowed comparison of rocks with varying compositions, porosities, and kerogen contents but with identical postdepositional histories. Most analyses were of finely laminated kerogenous shales from the Roy Hill Shale and Marra Mamba Formation that were deposited in a marine continental-slope environment below storm-wave base under suboxic conditions (*12*). Those from the Marra Mamba Formation were interbedded with oxide-facies banded iron formation. Black chert from the Warrie Member, quartz sandstone and vein dolomite from the Roy Hill Member, and terrestrial basalt from the Maddina Formation served as controls for laboratory procedures.

Although these rocks are well-preserved by Archean standards, they are nevertheless

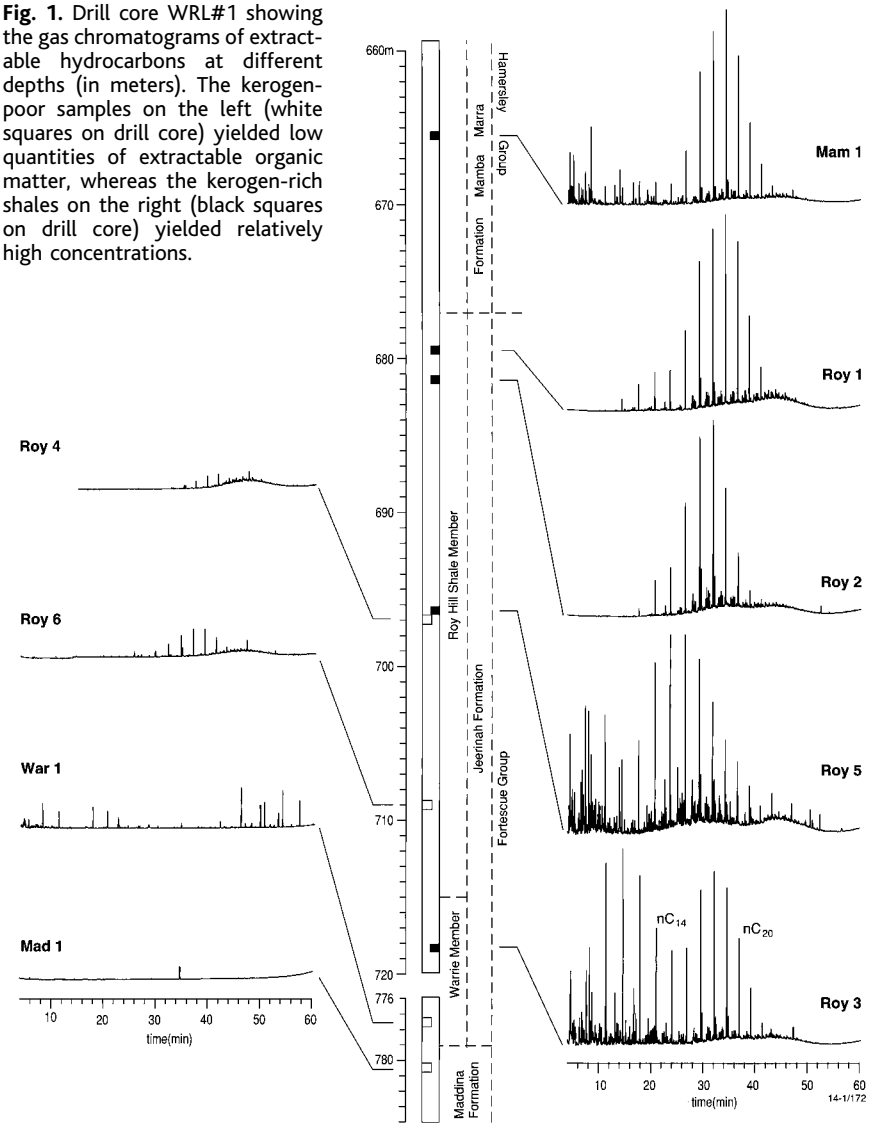

Fig. 1. Drill core WRL#1 showing the gas chromatograms of extractable hydrocarbons at different depths (in meters). The kerogen-poor samples on the left (white squares on drill core) yielded low quantities of extractable organic matter, whereas the kerogen-rich shales on the right (black squares on drill core) yielded relatively high concentrations.

[1]School of Geosciences, University of Sydney, Sydney, NSW 2006, Australia. [2]Australian Geological Survey Organisation (AGSO), Canberra, ACT 2601, Australia.

*To whom correspondence should be addressed. E-mail: jochen.brocks@agso.gov.au or brocks@es.su.oz.au

highly mature and therefore contain only small quantities of extractable hydrocarbons. Hence, they are especially prone to modern contamination by petroleum products during drilling, storage, and analysis. Accordingly, each sample underwent three solvent rinses to ensure that extracted bitumen was intimately associated with the rock and not superficial or lining cracks. After each rinse was analyzed chromatographically, the rock was broken into smaller fragments to expose fresh bedding surfaces, fractures, and fissures. If the last rinse proved clean, the sample was then finely ground and exhaustively extracted. The kerogenous shales yielded >25 μg of saturated hydrocarbons per gram of rock, 50 to 500 times more than the concentrations obtained from the chert and basalt and 50,000 times greater than laboratory system blanks (Table 1). The low hydrocarbon contents of the sandstone and vein dolomite represent traces of oil expelled from directly adjacent shales. Because modern petrochemical contamination should produce similar hydrocarbon distributions in all samples, the marked variations in these (Fig. 1) indicate that the extracted hydrocarbons are indeed indigenous.

Table 1. Kerogen and bitumen contents of WRL#1 samples. TOC, total organic carbon. n.m., not measured.

Sample	AGSO number	Depth (m)	Lithology	TOC (%)	Saturates (μg/g of rock)
Mam1	9983	665.39	Sideritic brown shale	2.6	28
Roy1	9710 8284	679.39	Pyritic black shale	7.4	36
Roy2	9710 8285	681.90	Pyritic black shale	8.6	26
Roy5	1999 0333	696.92*	Pyritic black shale	n.m.	>25
Roy4	1999 0331	696.94	Pyritic quartz sandstone	–	8
Roy6	1999 0332	709.59	Fibrous vein dolomite	–	5
Roy3	9984	718.23	Pyritic black shale	9.0	27
War1	9982	777.86	Massive black chert	0.5	0.6
Mad1	9985	780.65	Amygdaloidal basalt	–	0.07
Blank	–	–	–	–	0.0004†

*A 2-mm-thick layer on top of Roy4. †Referring to 100 g of rock.

Table 2. Abundances and isotopic compositions of kerogens and individual compounds. Biomarker ratios were measured according to published methods (*7, 15*). Numbers in subscript refer to the number of carbon atoms in the biomarker.

	Mam1	Roy1	Roy2	Roy5	Roy3
Depth (m)	665.4	679.4	681.9	696.9	718.2
Acyclic hydrocarbons*					
Pristane/phytane	1.2 (0.1)†	1.3	1.3	1.0	1.3
Pristane/*n*-C_{17}	0.2 (0.1)	0.3	0.4	0.5	0.3
Phytane/*n*-C_{18}	0.1 (0.1)	0.2	0.3	0.5	0.2
Hopanes‡ (ppm)§	230	300	75	–	110
$C_{27}Ts/(C_{27}Ts+C_{27}Tm)$‖	0.59 (0.01)	0.57	0.59	0.56	0.58
$C_{29}Ts/C_{29}$‖	0.23 (0.04)	0.24	0.16	0.20	0.25
$(C_{27}Ts+C_{27}Ts)/C_{29}$ ‖,¶	1.3 (0.40)	1.1	0.57	1.0	1.82
C_{29}/C_{30}¶	1.3 (0.20)	1.3	2.1	1.4	0.9
C_{30}/C_{31}¶	1.1 (0.16)	1.4	1.5	1.3	1.5
2α-Methylhopane index ¶,#	14 (1.4)	12	17	12	12
Steranes/Hopanes ‖,¶,**	0.79 (0.20)	0.95	2.6	0.61	1.1
Steranes (ppm)§	180	280	190	–	120
Dia- /Regular ‖,¶,††	0.58 (0.10)	0.91	1.33	0.77	0.87
C_{29} 20S/(20S+20R)‖	0.53 (0.04)	0.64	0.77	0.63	0.57
C_{29} αββ/(ααα+αββ)‖	0.54 (0.02)	0.58	0.63	0.61	0.57
$C_{27}/(C_{27}+C_{28}+C_{29})$¶	0.52 (0.03)	0.54	0.57	0.50	0.55
$C_{28}/(C_{27}+C_{28}+C_{29})$¶	0.21 (0.04)	0.19	0.20	0.20	0.20
$C_{29}/(C_{27}+C_{28}+C_{29})$¶	0.28 (0.04)	0.28	0.23	0.30	0.25
TA-I/(TA-I+TA-II) ‖,‡‡	0.92	0.94	0.96	>0.90	0.96
Carbon isotopes ($\delta^{13}C$ per mil PDB)					
Kerogen	−46.8§§	−39.5	−39.6	–	−41.1
n-C_{17}	−26.2‖‖	−26.2	−26.0	–	−27.0
n-C_{18}	−26.5	−26.1	−27.4	–	−26.3
Pristane	−28.8	−29.4	−29.8	–	−28.9
Phytane	−29.6	−29.5	−30.1	–	−27.8

*Ratios measured using GC-FID peak areas. †The value in parentheses is the maximum error of the particular ratio obtained in a series of repeat measurements. ‡$C_{27}Ts$ = 18α(H)-22,29,30-trisnorneohopane; $C_{27}Tm$ = 17α(H)-22,29,30-trisnorhopane; $C_{29}Ts$ = 18α(H)-30-norneohopane; C_{29} = 17α,21β(H)-30-norhopane; C_{30} = 17α,21β(H)-hopane; C_{31} = 22S + 22R 17β,21α(H)-29-homohopane; $2\alpha MeC_{31}$ = 2α-methyl-17α,21β(H)-hopane. §Estimated concentration of hopanes ($C_{27}Ts$, $C_{27}Tm$, $C_{29}Ts$, C_{29}, C_{30}, C_{31}, 2α-MeC_{31}) and steranes (C_{27} to C_{29} 20S + 20R 13β,17α(H)-diasteranes and C_{27} to C_{29} 20S + 20R 5α,14α,17α(H) and 5α,14β,17β(H)-regular steranes) in the saturated fraction of the bitumen. D_4-20R-5α,14α,17α(H)-cholestane was used as internal standard. ‖Indicates a parameter primarily controlled by degree of thermal maturation. ¶ Indicates a parameter primarily controlled by organic matter sources. #The $2\alpha\text{-}MeC_{31}/(2\alpha MeC_{31}+C_{30})$ is expressed as a percent. **Ratio measured using hopanes $C_{27}Ts$, $C_{27}Tm$, $C_{29}Ts$, C_{29}, C_{30}, C_{31} and the C_{27} to C_{29} dia- and regular steranes. ††Ratio measured using C_{27} to C_{29} 20S + 20R 13β,17α(H)-diasteranes and C_{27} to C_{29} 20S + 20R 5α,14α,17α(H) and 5α,14β,17β(H)-regular steranes. ‡‡Tri-aromatic-sterane ratios measured using SIR *m/z* 231 as defined in (*7*). §§Carbon isotope data measured by combustion of isolated kerogens (*4*). ‖‖ Analytical errors for GC-C-IRMS are within 0.4 per mil.

There are three potential sources of ancient but post-Archean organic contamination: local subsurface biological activity, groundwater carrying biolipids from the surface, and migrating petroleum carrying geolipids. The first two are easily excluded. Hydrous pyrolysis at 350°C of kerogens isolated from the shales Roy3 and Mam1 yielded insignificant quantities of hydrocarbon, as expected from highly mature Precambrian organic matter (*13*). Hydrocarbons extracted from these kerogens are also highly mature, based on the saturate and aromatic biomarker parameters conventionally used to assess thermal evolution (Table 2). This indicates that they were generated during the final stages of kerogen maturation, before or during peak metamorphism at 2450 to 2000 Ma (*14*). Because the rocks have not experienced a subsequent thermal event capable of turning immature biolipids into highly mature geolipids, the extracted hydrocarbons were not derived from post-Archean surface or subsurface biota.

Adulteration from migrating Phanerozoic or Proterozoic petroleum is harder to discount. The youngest rocks in the depositional basin belong to the ~2400-Ma Turee Creek Group. Younger petroleum-prone rocks were never deposited over the top of the basin in sufficient thickness for hydrocarbon expulsion to occur. The WRL#1 drill hole is located centrally within the craton, at least 150 km from the nearest post-Archean basin, so younger oils migrating laterally would have to travel long distances through deformed and metamorphosed Archean rocks without continuous cross-cutting fractures. Thus, the only likely source for adulterating oil is from older, rather than younger, rocks. Moreover, bedding-parallel permeability of the black shale Roy3 and pyritic sandstone Roy4 was below the detection limit of 0.01 millidarcy. Thus, these rocks might have been sealed to hydrocarbon migration since they were last metamorphosed at 2450 to 2000 Ma. Also, higher yields of bitumen from shales than from kerogen-poor rocks (Table 1, Fig. 1) are inconsistent with staining by migrated oil, which would have equally tainted all rocks of similar permeability. Notably, typical Phanerozoic geochemical characters, such as biomarkers derived from higher plants, are absent. However, isoalkanes are abundant, as in many Proterozoic bitumens (*15*, *16*), and the *n*-alkane distribution has a diminution in relative abun-

dance at the n-C_{22} homolog (Fig. 1), a pattern not observed in younger bitumens.

The strongest argument for hydrocarbon syngeneity is the variation in biomarker distributions between closely spaced shale samples (Table 2). The sterane:hopane ratio and 2α-methylhopane index are both gauges of different biological inputs during sedimentation, as are the ratios of sterane and hopane homologs. These differences among biomarker ratios cannot be explained by water washing, biodegradation, thermal degradation, or geochromatography of a homogeneous migrated oil. The observed variation is instead consistent with the diversity of syngenetic bitumen typically present within source rock facies.

To provide clues about organic origins, carbon isotopic ratios were measured for bulk kerogen and for individual hydrocarbons. Kerogens are depleted in ^{13}C as is typical of rocks of this age, with values of $\delta^{13}C$ falling between −40 and −47 per mil (Table 2). The $\delta^{13}C$ values for 12- to 22-carbon (C_{12}-C_{22}) n-alkanes range from −26 to −29 per mil. This enrichment in ^{13}C relative to kerogen is very rare in Phanerozoic kerogen-bitumen pairs but typical of, though more extreme than, other Precambrian samples (*17, 18*)—for example, the 600-Ma Pertatataka Formation where C_{16}-C_{20} n-alkanes are up to 6 per mil heavier than kerogen (*19*). It indicates that the organisms forming most of the kerogen did not contribute significantly to the n-alkanes. The isoprenoids pristane and phytane are depleted in ^{13}C relative to n-alkyl C_{17} and C_{18} compounds by ~3 per mil (Table 2), as in other analyses of Precambrian bitumen (*18*). The n-alkanes are probably the products of a diverse biota of primary producers and heterotrophs. The isoprenoids are derived from photosynthetic microbes with a possible contribution from isotopically light methanogenic Archaea, which are known to yield only small quantities of pristane and phytane relative to total biomass and no n-alkanes when pyrolyzed (*20*). The contrasting depletion of ^{13}C in the kerogen may be attributed to contributions from methanotrophs, as proposed by Hayes (*21*). However, n-alkanes derived from isotopically depleted membrane lipids of methanotrophs could not be identified in our samples. Furthermore, we cannot discount the possibility that the observed isotopic pattern could also reflect the products of an extinct biochemistry.

More information about biological precursors can be obtained from the tetracyclic and pentacyclic terpane biomarkers in the hydrocarbon extracts (Fig. 2). Until now, evidence for cyanobacteria in the Archean has been equivocal, based on poorly preserved microfossils (*22*) and on indirect geochemical arguments (*23*). High concentrations of 2α-methylhopanes (Table 2), also observed in other Precambrian and early Paleozoic sediments and apparently of cyanobacterial origin (*24*), are consistent with the early appearance of these organisms. Since oxygenic photosynthesis is their preferred physiology, metabolic oxygen excretion was evidently occurring well before significant oxygen had accumulated in the atmosphere, at about 2000 Ma (*25*). The abundance of cyanobacterial biomarkers in the Marra Mamba Formation, a unit predominantly consisting of oxide-facies banded iron formation, suggests that although Precambrian iron formations could have been produced by abiotic photochemical processes (*26*) or anoxygenic phototrophic bacteria (*27*), those in the Hamersley Group probably formed as a result of biogenic oxygen production (*28*).

Steranes also occur in the extracted bitumens (Fig. 2). They comprise most of the known C_{26} to C_{30} pseudohomologs, their aromatic counterparts, and A-ring methylated steranes that have been recorded in younger sediments. The biosynthesis of these sterols is characteristic of eukaryotes. The only prokaryotes known to synthesize sterols have biosynthetic pathways that stop short of cholesterol (*29*) or exclusively produce C_{27} cholestenols (*30*). Although it is possible that other yet unknown or extinct prokaryotes also produced sterols, the wide structural range of steranes, in relative abundances like those of younger bitumen, is convincing evidence for the presence of eukaryotes in the late Archean. The phylogenetic position of these eukaryotes remains unclear. The curtailed n-alkane distribution indicates that contributions from polymethylenic chains, derived from algal cell wall components (algaenans), were much lower than observed in younger marine sediments or were missing. We conclude that the domain Eucarya first appeared before 2700 Ma and is at least 500 to 1000 My older than indicated by current paleontological data (*31*). This age should provide a new calibration point for molecular clocks and the universal tree of life.

The biomarkers we report are the oldest known that are demonstrably indigenous and syngenetic. They are more than a billion years older than those from the ~1640-Ma Barney Creek Formation (*15*), previously the oldest well-characterized molecular fossils. Their dis-

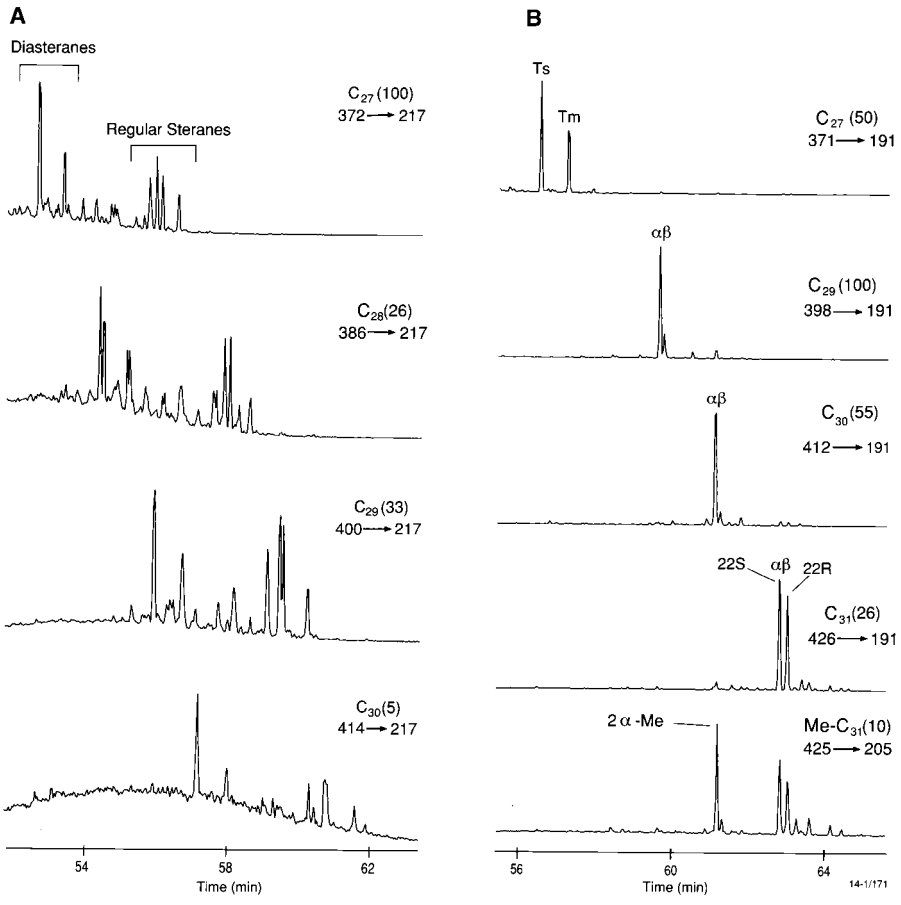

Fig. 2. Distribution of (**A**) sterane and (**B**) hopane hydrocarbons from Roy1. The data are MRM (multiple reaction monitoring) chromatograms obtained by gas chromatography–mass spectrometry (GC-MS) analysis of metastable molecular ions fragmenting to daughter ions at mass-to-charge ratio (m/z) = 217 for steranes, m/z = 191 for hopanes, and m/z = 205 for methylhopanes. Chromatograms are identified by carbon numbers, the relative height (abundance) of the most intense peak in the trace, and the reaction transition.

tinctive features are very similar to those observed in the ~2500-Ma Mt. McRae Shale, and their age is supported by more thorough analytical protocols (*24*). The discovery and careful analysis of biomarkers in rocks of still greater age and of different Archean environments will potentially offer new insights into early microbial life and its evolution.

References and Notes

1. J. W. Schopf, *Science* **260**, 640 (1993).
2. M. R. Walter, in *Earth's Earliest Biosphere*, J. W. Schopf, Ed. (Princeton Univ. Press, Princeton, NJ, 1983), pp. 187–213.
3. S. J. Mojzsis *et al.*, *Nature* **384**, 55 (1996).
4. J. M. Hayes, I. R. Kaplan, K. W. Wedeking, in (*2*), pp. 93–134.
5. F. D. Mango, *Nature* **352**, 146 (1991).
6. A. Dutkiewicz, B. Rasmussen, R. Buick, *ibid.* **395**, 885 (1998).
7. K. E. Peters and J. M. Moldowan, *The Biomarker Guide* (Prentice-Hall, Englewood Cliffs, NJ, 1993).
8. R. C. Morris, *Precambrian Res.* **60**, 243 (1993).
9. A. F. Trendall, D. R. Nelson, J. R. de Laeter, S. W. Hassler, *Aust. J. Earth Sci.* **45**, 137 (1998).
10. N. T. Arndt, D. R. Nelson, W. Compston, A. F. Trendall, A. M. Thorne, *ibid.* **38**, 261 (1991).
11. R. E. Smith, J. L. Perdrix, T. C. Parks, *J. Petrol.* **23**, 75 (1982).
12. J. M. Gressier, thesis, University of Sydney, Sydney, Australia (1996).
13. T. C. Hoering and V. Navale, *Precambrian Res.* **34**, 247 (1987).
14. D. R. Nelson, A. F. Trendall, J. R. de Laeter, N. J. Grobler, I. R. Fletcher, *ibid.* **54**, 231 (1992).
15. R. E. Summons, T. G. Powell, C. J. Boreham, *Geochim. Cosmochim. Acta* **52**, 1747 (1988).
16. R. E. Summons and M. R. Walter, *Am. J. Sci.* **290A**, 212 (1990).
17. T. C. Hoering, *Carnegie Inst. Wash. Yearb.* **64**, 215 (1965); *ibid.* **65**, 365, (1966).
18. G. A. Logan, J. M. Hayes, G. B. Heishima, R. E. Summons, *Nature* **376**, 53 (1995); G. A. Logan, R. E. Summons, J. M. Hayes, *Geochim. Cosmochim. Acta* **61**, 5391 (1997).
19. G. A. Logan *et al.*, *Geochim. Cosmochim. Acta*, **63**, 1345 (1999).
20. S. J. Rowland, *Org. Geochem.* **15**, 9 (1990).
21. J. M. Hayes, in *Early Life on Earth*, Nobel Symposium No. 84, S. Bengtson, Ed. (Columbia Univ. Press, New York, 1994), pp. 220–236.
22. J. W. Schopf and B. M. Packer, *Science* **237**, 70 (1987).
23. R. Buick, *ibid.* **255**, 74 (1992).
24. R. E. Summons, L. L. Jahnke, J. M. Hope, G. A. Logan, *Nature*, in press.
25. H. D. Holland and N. J. Beukes, *Am. J. Sci.* **290A**, 1 (1990); A. H. Knoll and H. D. Holland, in *Effects of Past Global Change on Life*, S. M. Stanley, Ed. (National Academy Press, Washington, DC, 1995), pp. 21–33.
26. P. S. Braterman, A. G. Cairns-Smith, R. W. Sloper, *Nature* **303**, 163 (1983).
27. F. Widdel *et al.*, *ibid.* **362**, 834 (1993).
28. P. Cloud, *Science* **160**, 729 (1968); *Econ. Geol.* **68**, 1135 (1973).
29. G. Ourisson, M. Rohmer, K. Poralla, *Annu. Rev. Microbiol.* **41**, 301 (1987).
30. W. Kohl, A. Gloe, H. Reichenbach, *J. Gen. Microbiol.* **129**, 1629 (1983).
31. T.-M. Han and B. Runnegar, *Science* **257**, 232 (1992); A. H. Knoll, *ibid.* **256**, 622 (1992).

32. Supported by the Studienstiftung des Deutschen Volkes (J.J.B.) and American Chemical Society Petroleum Research Fund (R.B.). We thank J. Gressier and RioTinto Exploration for samples, the AGSO Isotope & Organic Geochemistry staff for technical assistance, J. Kamprad for x-ray diffraction analyses, T. Blake, D. Des Marais, L. L. Jahnke, C. J. Boreham, D. S. Edwards, T. G. Powell, D. E. Canfield, and M. R. Walter for advice, and J. M. Hayes, A. Knoll, and an anonymous reviewer for their thoughtful comments. G.A.L. and R.E.S. publish with the permission of the Executive Director of AGSO.

19 May 1999; accepted 13 July 1999

REPORTS

Josephson Persistent-Current Qubit

J. E. Mooij,[1,2]* T. P. Orlando,[2] L. Levitov,[3] Lin Tian,[3] Caspar H. van der Wal,[1] Seth Lloyd[4]

A qubit was designed that can be fabricated with conventional electron beam lithography and is suited for integration into a large quantum computer. The qubit consists of a micrometer-sized loop with three or four Josephson junctions; the two qubit states have persistent currents of opposite direction. Quantum superpositions of these states are obtained by pulsed microwave modulation of the enclosed magnetic flux by currents in control lines. A superconducting flux transporter allows for controlled transfer between qubits of the flux that is generated by the persistent currents, leading to entanglement of qubit information.

In a quantum computer, information is stored on quantum variables such as spins, photons, or atoms (*1*–*3*). The elementary unit is a two-state quantum system called a qubit. Computations are performed by the creation of quantum superposition states of the qubits and by controlled entanglement of the information on the qubits. Quantum coherence must be conserved to a high degree during these operations. For a quantum computer to be of practical value, the number of qubits must be at least 10^4. Qubits have been implemented in cavity quantum electrodynamics systems (*4*), ion traps (*5*), and nuclear spins of large numbers of identical molecules (*6*). Quantum coherence is high in these systems, but it seems difficult or impossible to realize the desired high number of interacting qubits. Solid state circuits lend themselves to large-scale integration, but the multitude of quantum degrees of freedom leads in general to short decoherence times. Proposals have been put forward for future implementation of qubits with spins of individual donor atoms in silicon (*7*), with spin states in quantum dots (*8*), and with d-wave superconductors (*9*); the technology for practical realization still needs to be developed.

[1]Department of Applied Physics and Delft Institute for Microelectronics and Submicron Technologies, Delft University of Technology, Post Office Box 5046, 2600 GA Delft, Netherlands. [2]Department of Electrical Engineering and Computer Science, [3]Department of Physics and Center for Materials Science and Engineering, [4]Department of Mechanical Engineering, Massachusetts Institute of Technology, Cambridge, MA 02139, USA.

*To whom correspondence should be addressed. E-mail: mooij@qt.tn.tudelft.nl

In superconductors, all electrons are condensed in the same macrosopic quantum state, separated by a gap from the many quasi-particle states. This gap is a measure for the strength of the superconducting effects. Superconductors can be weakly coupled with Josephson tunnel junctions (regions where only a thin oxide separates them). The coupling energy is given by $E_J(1 - \cos \gamma)$, where the Josephson energy E_J is proportional to the gap of the superconductors divided by the normal-state tunnel resistance of the junction and γ is the gauge-invariant phase difference of the order parameters. The current through a Josephson junction is equal to $I_o \sin \gamma$, with $I_o = (2e/\hbar) E_J$, where e is the electron charge and $\hbar$ is Planck's constant divided by 2π. In a Josephson junction circuit with small electrical capacitance, the numbers of excess Cooper pairs on islands n_i, n_j and the phase differences γ_i, γ_j are related as noncommuting conjugate quantum variables (*10*). The Heisenberg uncertainty between phase and charge and the occurrence of quantum superpositions of charges as well as phase excitations (vortexlike fluxoids) have been demonstrated in experiments (*11*). Coherent charge oscillations in a superconducting quantum box have recently been observed (*12*). Qubits for quantum computing based on charge states have been suggested (*13*, *14*). However, in actual practice, fabricated Josephson circuits exhibit a high level of static and dynamic charge noise due to charged impurities. In contrast, the magnetic background is clean and stable. Here, we present the design of a qubit with persistent currents of opposite sign as its basic states. The qubits